Ceramics-Silikáty 67 (1), 64-72 (2023)
www.ceramics-silikaty.cz doi: 10.13168/cs.2023.0003

# SYNERGISTIC ACTIVATION OF MANUFACTURED SAND POWDER-SLAG-GYPSUM CEMENTITIOUS COMPOSITES USING RESPONSE SURFACE METHODOLOGY

ZHANG HAOLI*, #CHEN WEI*, XU YIDONG*, **, WANG JIALEI*, WANG RUI*, WU PING*, WU JINTING*

*School of Civil Engineering and Architecture, NingboTech University, Ningbo 315100, China
**School of Civil Engineering, Chongqing Jiaotong University, Chongqing 400074, China

#E-mail: chenw@nit.zju.edu.cn

Submitted November 7, 2022; accepted January 12, 2023

**Keywords:** Synergistic activation, Multiple composite, Response surface method, Mechanical properties

*The synergistic effects of alkali and sulfate activators on the flexural and compressive strengths of manufactured cementitious composites comprising slag, fly ash and cement were studied in the present manuscript. The experimental procedure used a central composite design (CCD) for the response surfaces. A regression model was established and tested with the experimental results. The maximum flexural strength, compressive strength, and stone powder content at each age were used as the target values for optimisation. The optimal mixing proportion included 14.45 % manufactured sand powder and 0.91 % gypsum. In addition, the effects of the sulfate activator on the manufactured sand powder-slag-gypsum cementitious composite (MSGCC) hydration were analysed after 1 and 3 days, and the mechanism for the synergistic activation of MSGCC by alkali and sulfate activators was elucidated upon/clarified.*

## INTRODUCTION

Stone powder is a by-product of stone crushing during the production process for machine-made sand. The State Council issued the Action Plan for Achieving Carbon Peak before 2030. The plan supports the large-scale utilisation of solid waste, such as mineral powder, stone powder, fly ash, industrial gypsum by-products and construction waste, to replace non-renewable resources, such as natural sand and stone. The procedure strongly promotes the application and development of machine-made sand and stone powder. Stone powder is usually used as a concrete admixture. However, due to its poor hydration and pozzolanic activity, excessive mixing significantly decreases the strength, generally to less than 10 % [1-3], lacks effective utilisation and results in large amounts of accumulated stone powder. The issue of prompt stone powder treatment needs to be addressed.

Many studies [4-10] have shown that industrial waste, such as slag and fly ash, have a potential activity capacity and can be used to prepare effective binders with alkali activators. These low-carbon binders have the advantages of a high early strength and good durability. In addition, sulfate is also an important source of activation. Sulfate activators include sodium sulfate, gypsum, etc. [11-14]. When a sulfate activator is used alone, the activity of the waste residue cannot be fully stimulated, but the sulfate activation effect can be significantly improved in alkaline environments [15, 16]. Lv [17] found that when sodium silicate was used to activate fly ash, a high sodium sulfate content was conducive to the formation of sodium alumina silicate hydrate (N-A-S-H), promoted microstructural development and significantly improved the strength; while a low content had no significant effect. Lei [18] showed that with sulfate-activated slag, the 28-day compressive strength of 40 % ordinary Portland cement reached 46 MPa, which was similar to the strength of a pure cement slurry. Based on the existing research, the combined use of alkali and sulfate activators with waste residue may produce better results and improve the properties of cementitious materials.

The response surface method (RSM) is a statistical method that leads to optimal parameters by establishing regression models and analysing them. It has advantages, such as fewer tests, high precision, and the ability to analyse interactions [19-21]. In this paper, the response surface method (RSM) was used to study the effects of stone powder and a sulfate activator on a composite cementitious material based on stone powder-slag-gypsum; the alkali and sulfate activation were combined to study the effects of the stone powder and sulfate activator on the composite cementitious material and obtain the optimal mixing ratio. The activation mechanism for the sulfate activator with multiplex cementitious materials was analysed from the two perspectives of hydration heat and hydration products and provides a reference for activation studies with other multiplex composite systems.

## EXPERIMENTAL

### Raw material

(1) The composition of the blast furnace slag powder (Grade S95 slag powder, Ningbo Ziheng Building Materials Technology Co., LTD) used in this study is shown in Table 1.

Table 1. Chemical composition of the slag powder.

| Chemical component | CaO | $SiO_2$ | $Al_2O_3$ | $Na_2O$ | $SO_3$ | $K_2O$ | $TiO_2$ | MnO | $Fe_2O_3$ |
|---|---|---|---|---|---|---|---|---|---|
| Content (%) | 35.93 | 30.74 | 17.55 | 0.40 | 0.26 | 2.76 | 1.21 | 0.38 | 0.84 |

(2) The stone powder was a tuff stone powder with an apparent density of 2.636 g·cm$^{-3}$ and was produced from Dahuangshan Mountain, Zhoushan Island; its main chemical composition is shown in Table 2.

Table 2. Chemical composition of the tuff powder.

| Chemical component | CaO | $SiO_2$ | $Al_2O_3$ | $Na_2O$ | $SO_3$ | $K_2O$ | $TiO_2$ | MnO | $Fe_2O_3$ |
|---|---|---|---|---|---|---|---|---|---|
| Content (%) | 2.98 | 63.56 | 15.69 | 3.42 | 0.26 | 2.76 | 0.65 | 0.32 | 5.48 |

(3) The cement was Panlongshan (brand P. I Portland cement) with a strength grade of 52.5; it was produced by the Shandong Kangjing New Material Technology Co., LTD.

(4) The fly ash was Grade II and was produced by the Lingshou County Languo Mineral Products Processing Plant.

(5) The alkali activator was liquid sodium silicate produced by the Jiashan Yourui Refractory Co., Ltd. The product parameters are shown in Table 3. The solid sodium hydroxide was analytically pure and flake-shaped with a content ≥ 99.0 %; it was produced by the Wuxi Jinko Chemical Co., LTD.

Table 3. Sodium silicate parameters.

| $SiO_2$ (%) | $Na_2O$ (%) | Baume degree/20 °C | Modulus |
|---|---|---|---|
| 27.3 | 8.54 | 38.5 Be | 3.3 |

(6) The sulfate activator was gypsum produced by the Gongyi Yuanheng Water Purification Materials Factory.

(7) The sand was ISO (the International Organization for Standardization) standard sand produced by the Xiamen Aisiou Standard Sand Co., Ltd.

(8) The water used was tap water.

### Experimental design

The mixture was composed of the mineral powder, stone powder, fly ash, cement, alkali activator and gypsum, and the contents of the cement, fly ash and alkali activator were fixed. With the stone sand powder content (x1) and gypsum content (x2) as the test factors and the 1-d bending strength (y1), 3-d bending strength (y2), 28-d bending strength (y3), 1-d compressive strength (y4), 3-d compressive strength (y5) and 28-d compressive strength (y6) as the RSM values, Design Expert software was used to design a two-factor and five-level central composite design (CCD) for a total of 13 test sites. Based on previous tests and the existing research results [22, 23], the test factors and levels are shown in Table 4.

Table 4. Test factors and levels.

| Factor | Level | | | | |
|---|---|---|---|---|---|
| | -1.414 | -1 | 0 | 1 | 1.414 |
| Powder content (x1) (%) | 6.89 | 10.00 | 17.50 | 25.00 | 28.11 |
| Gypsum content (x2) (%) | 0.19 | 0.50 | 1.25 | 2.00 | 2.31 |

### Specimen preparations and test methods

Initially, certain amounts of water and sodium hydroxide were added to the water glass, then stirred and dissolved; the required modulus of the alkali activator was prepared and allowed to dry for a day. The next day, the powder was weighed, poured into a mixing pot and stirred well. Then, the alkali activator was poured into the solution and stirred again. Next, the solution was poured into a mould (40 × 40 × 160 mm), which was vibration moulded and placed into a standard curing room. Finally, the mould was released after 24 h and placed into water for standard curing to the corresponding age. The preparation process is shown in Figure 1.

The flexural and compressive strengths were determined by using the Test Method of Cement Mortar Strength (ISO Method) (GB/T17671-1999). An STYE-300E digital display cement flexural and compressive instrument produced by Zhejiang Tugong Instrument Manufacturing Co., LTD, was used for the strength analyses.

## RESULTS AND DISCUSSION

### Experimental results and model building

According to the test design scheme, there were 13 groups of mixing ratios and three instars; 39 groups of tests were completed. The strength test results for the different instars are shown in Table 5. The experimental data were processed with the Design Expert software, the model was selected, and multiple regression equations

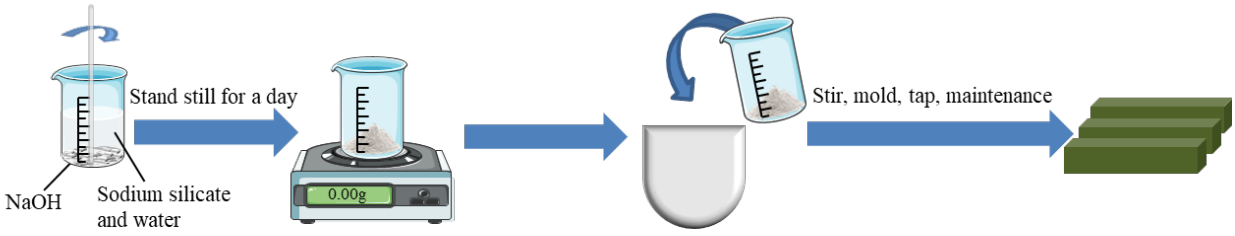


Figure 1. Sample preparation process.

were obtained through the analyses, as shown in Equations 1-6. Finally, variance analyses were conducted on the regression equations, and the results are shown in Table 6 and Table 7.

$$y1 = 2.62311 + 0.30828\,x1 + 1.96650\,x2 - 0.022222\,x1\,x2 - 0.0092\,x1^2 - 0.52\,x2^2 \quad (1)$$

$$y2 = 7.16820 + 0.038581\,x1 + 1.10286\,x2 - 0.00888889\,x1\,x2 - 0.00242222\,x1^2 - 0.46444\,x2^2 \quad (2)$$

$$y3 = 7.80695 - 0.025412\,x1 + 1.23754\,x2 - 0.00888889\,x1\,x2 - 0.0000666667\,x1^2 - 0.49556\,x2^2 \quad (3)$$

$$y4 = 44.98765 - 0.54365\,x1 - 1.45592\,x2 \quad (4)$$

$$y5 = 64.11468 - 0.37040\,x1 - 2.55543\,x2 \quad (5)$$

$$y6 = 84.94844 - 0.39770\,x1 - 2.42782\,x2 \quad (6)$$

Table 6. Analysis of the variance for the flexural strength.

| RSM | y1 | y2 | y3 |
|---|---|---|---|
| Model | | | |
| F value | 11.21 | 16.13 | 22.46 |
| P value | 0.0031 | 0.0010 | 0.0004 |
| Lack of Fit | 0.1180 | 0.4845 | 0.1833 |
| $R^2$ | 0.8890 | 0.9201 | 0.9413 |
| C.V.% | 4.20 | 2.28 | 1.41 |
| Adeq Precision | 8.810 | 12.120 | 15.397 |
| P value (factors) | | | |
| x1 | 0.0091 | 0.0002 | 0.0001 |
| x2 | 0.0482 | 0.0298 | 0.0189 |
| x1x2 | 0.3442 | 0.5676 | 0.3918 |
| $x1^2$ | 0.0009 | 0.0681 | 0.9306 |
| $x2^2$ | 0.0166 | 0.0044 | 0.0003 |

The regression model results showed that the F values for the flexural and compressive strengths at each age (y1, y2, y3, y4, y5, and y6) were 11.21, 16.13, 22.46, 112.54, 58.20 and 54.20, respectively. The P values were all less than 0.05, indicating that the model was significant. The P values of the missing fitting terms were all greater than 0.05, which indicated that the values predicted by the model significantly correlated with the experimental data, and the fits were good. The $R^2$ values for y1, y2, y3, y4, y5, and y6 were 0.8890, 0.9201, 0.9413, 0.9575, 0.9209 and 0.9155, respectively; these were close to 1, indicating the high accuracy of the model. The C.V.% values (y1, y2, y3, y4, y5, and y6) were 4.20, 2.28, 1.41, 2.36, 1.63 and 1.27, respectively; these were all less than 10 and indicated small degrees of data dispersion. The precision values were 8.810, 12.120, 15.397, 30.167,

Table 7. Analysis of the variance for the compressive strength.

| RSM | y4 | y5 | y6 |
|---|---|---|---|
| Model | | | |
| F value | 112.54 | 58.20 | 54.20 |
| P value | < 0.0001 | < 0.0001 | < 0.0001 |
| Lack of Fit | 0.1217 | 0.3446 | 0.2026 |
| $R^2$ | 0.9575 | 0.9209 | 0.9155 |
| C.V.% | 2.36 | 1.63 | 1.27 |
| Adeq Precision | 30.167 | 22.091 | 21.067 |
| P value (factors) | | | |
| x1 | < 0.0001 | < 0.0001 | < 0.0001 |
| x2 | 0.0031 | 0.0001 | 0.0003 |

Table 5. Test design and results

| Number | Powder content (x1) (%) | Gypsum content (x2) (%) | Flexural strength (MPa) | | | Compressive strength (MPa) | | |
|---|---|---|---|---|---|---|---|---|
| | | | 1-d (y1) | 3-d (y2) | 28-d (y3) | 1-d (y4) | 3-d (y5) | 28-d (y6) |
| 1 | 25.00 | 2.00 | 5.5 | 6.5 | 7.1 | 28.0 | 48.8 | 69.3 |
| 2 | 17.50 | 1.25 | 6.3 | 7.7 | 7.8 | 33.9 | 55.1 | 74.3 |
| 3 | 25.00 | 0.50 | 5.2 | 7.1 | 7.6 | 31.0 | 54.0 | 74.2 |
| 4 | 10.00 | 0.50 | 5.7 | 7.8 | 8.1 | 38.0 | 59.8 | 80.1 |
| 5 | 6.89 | 1.25 | 5.5 | 7.9 | 8.3 | 41.1 | 57.2 | 78.3 |
| 6 | 17.50 | 1.25 | 6.1 | 7.6 | 8.0 | 33.9 | 53.5 | 75.1 |
| 7 | 17.50 | 1.25 | 6.4 | 7.5 | 7.9 | 32.8 | 55.4 | 75.9 |
| 8 | 17.50 | 0.19 | 5.4 | 7.1 | 7.4 | 35.1 | 56.5 | 77.3 |
| 9 | 28.11 | 1.25 | 4.8 | 6.6 | 7.5 | 28.5 | 49.9 | 69.7 |
| 10 | 10.00 | 2.00 | 6.5 | 7.4 | 7.8 | 35.8 | 54.9 | 75.1 |
| 11 | 17.50 | 1.25 | 6.5 | 7.3 | 7.9 | 33.1 | 55.2 | 76.0 |
| 12 | 17.50 | 2.31 | 5.8 | 6.9 | 7.3 | 32.6 | 52.8 | 74.0 |
| 13 | 17.50 | 1.25 | 6.5 | 7.7 | 8.0 | 33.7 | 54.6 | 75.1 |

22.091 and 21.067; these were all greater than 4 and indicated that the model showed strong anti-interference capability. All the indices of the model were within a reasonable range, had strong reliability, and were used to analyse and predict the influence of the stone powder and gypsum on the strengths of the MSGCC at different ages.

## Interpretation of the results

The response surface map and contour map were drawn with the Design Expert software; these maps directly reflected the effects of the stone powder, gypsum and their interactions on the flexural and compressive strengths at each age, as shown in Figures 2-7. The distortion of the response surface and curvature of the contour line reflected the influence of the interactions on the flexural and compressive strengths of each age. A steeper response surface corresponded to the greater curvature of the contour and the more evident influence of the interaction [24, 25].

As shown in Figure 2, when the content of the stone powder was low (10 %), the 1-d flexural strength gradually increased with the increasing gypsum content, and the rate of increase for the trend slowed; when the content of the stone powder was high (25 %), the 1-d flexural strength initially increased and then decreased with the increasing gypsum content. This showed a parabolic trend with a relatively large decreasing amplitude. As shown in Figure 3, with an increase in the gypsum content, the 3-d flexural strength initially increased and then decreased and showed a relatively gentle parabolic trend. With an increase in the amount of stone powder, the 3-d flexural strength approximately linearly decreased with a large decline. As shown in

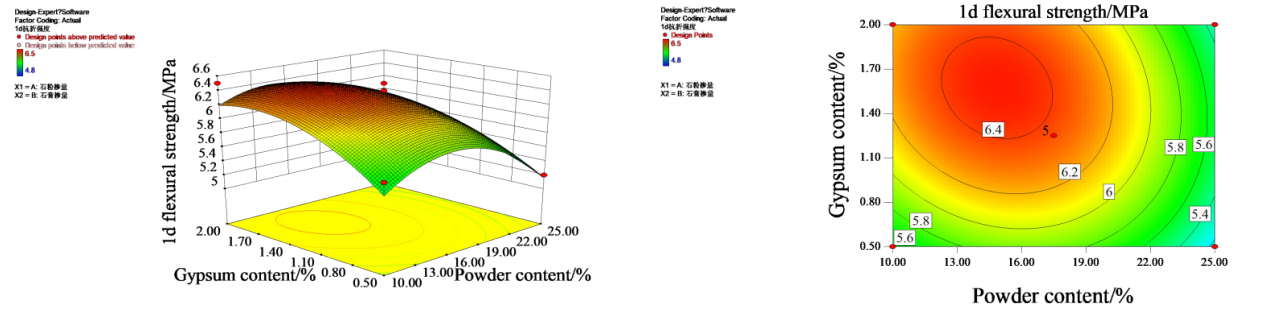


a) b)

Figure 2. Three-dimensional response surface and contour map for the 1-d flexural strength.

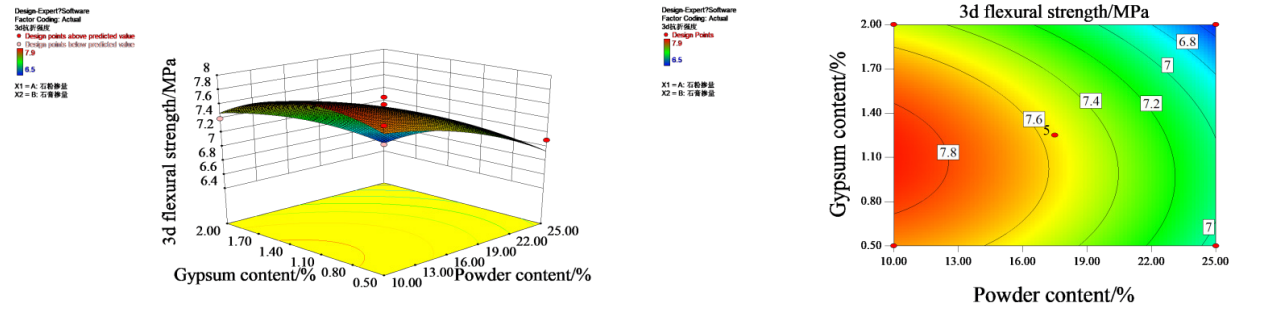


a) b)

Figure 3. Three-dimensional response surface and contour map for the 3-d flexural strength.

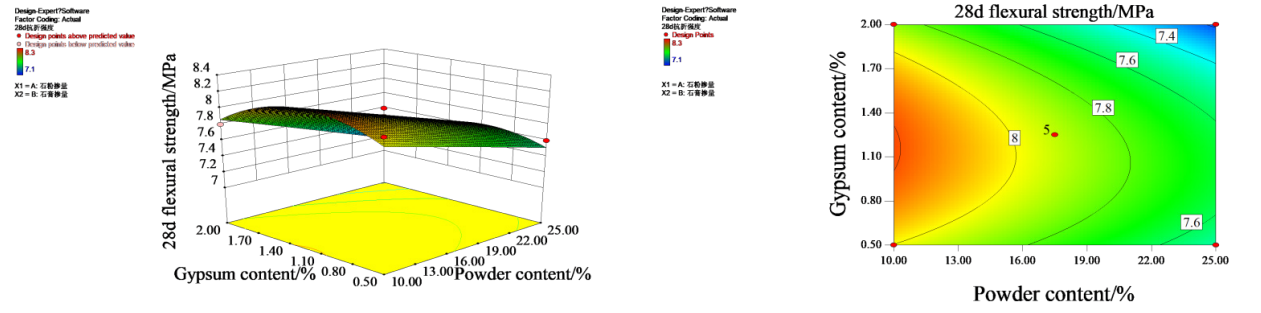


a) b)

Figure 4. Three-dimensional response surface and contour map for the 28-d flexural strength.

Figure 4, with an increase in the gypsum content, the 3-d flexural strength initially increased and then decreased and showed a relatively apparent parabolic trend. The 28-d flexural strength decreased linearly with the increasing stone powder content.

In addition, the response surface distortions were not evident in Figures 2-4; the contour curvatures were small and approximately circular, indicating that the interactions between the stone powder and gypsum had little influence on the bending strength. In the analysis of the variance results in Table 6, all the P values of the interaction terms are greater than 0.05, which verifies or confirms this result. As shown in Figures 5-7, the compressive strength of each age decreased linearly with the increasing amounts of stone powder and gypsum. All the response surfaces showed one plane without distortion, and the contours were almost parallel. A shown by the analysis of variance results in Table 7, the stone powder and gypsum had no effect on the compressive strength.

The above results showed that the stone powder had a negative effect on the strength of the MSGCC, but the strength did not decrease significantly; this indicated that the activity of the stone powder started when using both alkali and sulfate activation. The addition of an appropriate sulfate activator promoted the development of the bending strength, but it did not enhance the compressive strength. Liu [26] also found a similar trend. Within a certain gypsum content range, the trends for the compressive strength and bending strength of alkali-activated slag materials were inversely proportional.

A proper amount of stone powder can improve the strength of the cement and concrete, but excessive mixing causes adverse effects [1, 27-29]. Since neither fly

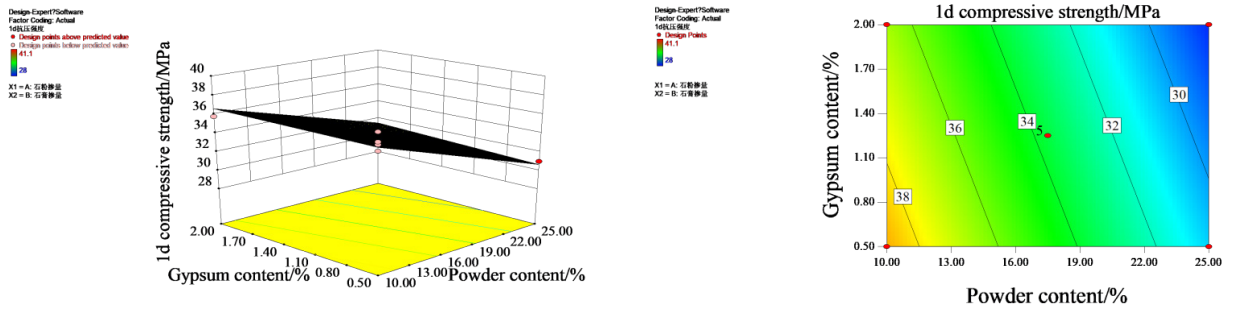


a) b)

Figure 5. Three-dimensional response surface and contour map for the 1-d compressive strength.

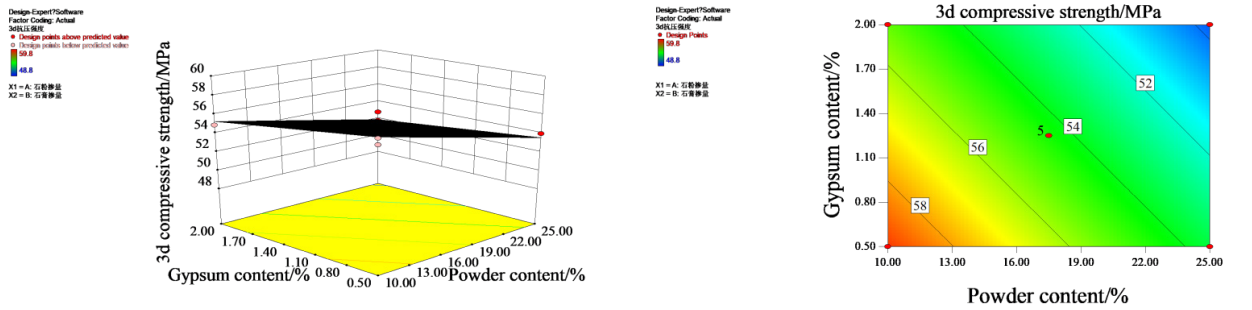


a) b)

Figure 6. Three-dimensional response surface and contour map for the 3-d compressive strength.

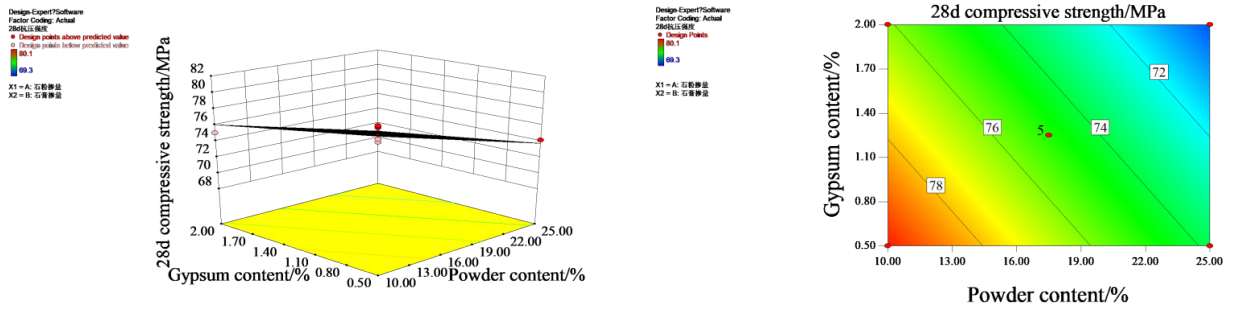


a) b)

Figure 7. Three-dimensional response surface and contour map for the 28-d compressive strength.

ash nor stone powder in the multicomponent composite cementing material prepared in this paper participated completely in the hydration reaction, the residual fly ash formed microaggregates to fill the internal pores of the material, which was similar to the effect of the residual stone powder. Therefore, the addition of stone powder to a certain amount of fly ash caused a decrease in the strength. Zhang Lanfang [22] believed that adding a small amount of gypsum to the alkali-activated system provided strength, but adding too much destroyed the material structure and reduced the strength. Nevertheless, cement was added to the multicomponent composite system in this study, and the cement contained a small amount of gypsum that was close to the optimal amount of gypsum; the gypsum adversely affected the strength. Alkali activators had a strong effect on the multicomponent composite system; large amounts of calcium silicate hydrate (C-S-H), N-A-S-H and other gels were generated in the reaction, while ettringite (Aft) was mainly generated by the sulfate activation. The synergistic effect of the two activators affected the overall structure of the multicomponent composite cementing material. At the micro level, gypsum provides activation in an alkaline environment, but excessive calcium inhibits the formation of N-A-S-H [30]. The N-A-S-H gel has a three-dimensional network structure, while the C-S-H gel has a chain structure, and they are not connected as an entire structure. Therefore, with an increasing gypsum content, within a certain range, the yield of the two gels changed, and the bending strength increased while the compressive strength decreased.

With the alkali activation, OH- destroyed the surfaces of the material particles, releasing active ions such as $Ca^{2+}$ to recombine and form gels such as C-S-H. With the sulfate activation, $OH^-$, $Ca^{2+}$, $SO_4^{2-}$, and $AlO^{2-}$ reacted to form AFt. The two activation effects operated together, and gypsum provided $Ca^{2+}$ and $SO_4^{2-}$; large amounts of calcium, silicon, aluminium and other phases were produced during the alkali activation process. On the one hand, the hydration processes of the two activation effects affect each other and improve the reaction environment; on the other hand, the two activation products are connected to each other, which improves their volume stability.

## Parameter optimisation and verification

To improve the utilisation rate of the stone powder, the maximum flexural strengths and compressive strengths of the stone powder after 1, 3 and 28 d were taken as the target values. Design Expert software was used to optimise the test factors, and the optimal ratios were obtained for the stone powder (14.45 %) and gypsum (0.91 %). The test results are shown in Table 8. The errors between the predicted and measured values for the flexural and compressive strength at each age were 2.96 %, 2.40 %, 0.38 %, and 4.25 %, 1.17 %, 0.22 %, respectively; these results indicated that the model selected by the response surface method was highly applicable and was used to predict the flexural and compressive strengths of MSGCC.

Table 8. Experimental verification of the best ratio·

| Response | | Predicted value (MPa) | Actual value (MPa) | Error (%) | Standard deviation |
|---|---|---|---|---|---|
| Flexural strength | 1 d | 6.22 | 6.41 | 2.96 | 0.25 |
| | 3 d | 7.72 | 7.91 | 2.40 | 0.17 |
| | 28 d | 8.02 | 7.99 | 0.38 | 0.11 |
| Compressive strength | 1 d | 35.81 | 34.35 | 4.25 | 0.80 |
| | 3 d | 56.45 | 57.12 | 1.17 | 0.88 |
| | 28 d | 77.00 | 76.83 | 0.22 | 0.95 |

## Mechanism of coactivation

### *Thermal analysis of hydration*

Using the optimal mix ratio analysed in Section 2, 14.45 % stone powder and three levels of gypsum (0 %, 1 %, 2 %) were combined to prepare the composite cementitious materials, and the effects of different sulfate activator dosages on the hydration process were investigated. The hydration heat release rates for 4 and 24 h are shown in Figures 8 and 9.

As shown in Figure 8, when using both the alkali and sulfate activation, the hydration reaction of the composite cementitious material was fast; it occurred within 4 h and shows two exothermic peaks. The first and second exothermic peaks appeared at approximately 20 and 90 min, respectively. The first exothermic peak decreased gradually with the addition of the sulfate activator, and the peak position remained unchanged. Compared with the base group (0 % sulfate activator), the two peaks formed with the addition of the 1 % sulfate activator were basically in the same location, but upon adding the 2 % sulfate activator, the exothermic peak decreased and shifted to the right. With the addition of

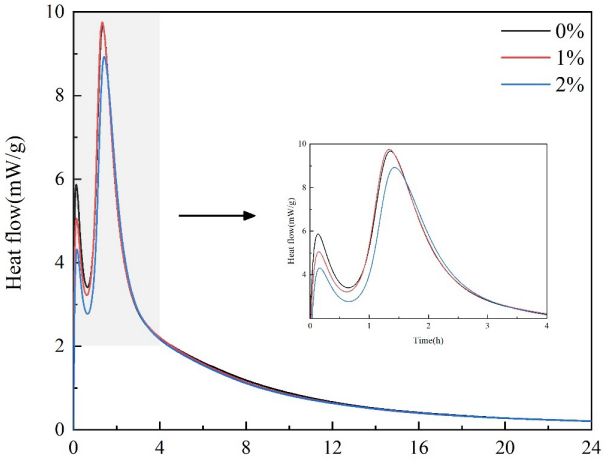


Figure 8. Hydration heat release rate for the MSGCC with the different gypsum contents.

the sulfate activator, the hydration induction stage was advanced, the hydration reaction entered the accelerated stage faster, and the peak width gradually narrowed. As shown in Figure 9, the hydration caloric release curves of the multi-compound cementitious materials with the 0 % and 1 % sulfate activator content remained basically unchanged in the first 2 hours, and the caloric release gap between 2 and 24 hours gradually expanded. The influence of the sulfate activator content on the cumulated hydration heat release decreased in the order 0 % > 1 % > 2 %. AFt was generated in the whole reaction process, covered the surfaces of the particles, slowed the hydration reaction and caused a decrease in the hydration heat release rate and heat release; AFt generation was the main reason for the decrease in strength.

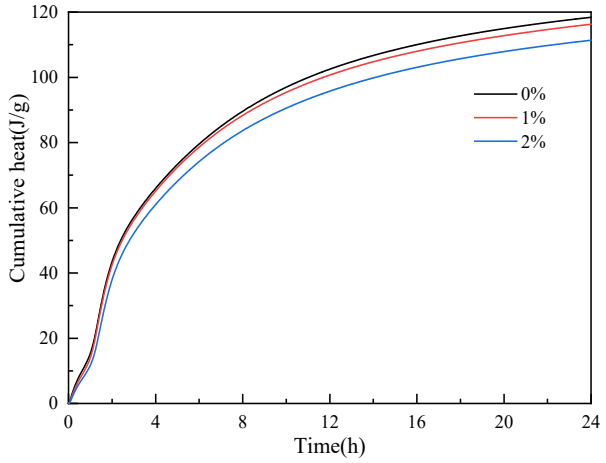


Figure 9. Hydration heat release for the MSGCC with the different gypsum contents.

*Analyses of hydration products*

Figure 10 shows the X-ray diffraction (XRD) patterns obtained after 1 and 3 d for the composite materials containing different gypsum contents, which demonstrated the effects of the sulfate activator (0 %, 1 %, 2 %) on the phase composition. As shown in Figure 10, the main crystalline phases seen after 1 d were quartz, gypsum and calcite. Among these, the sample with the sulfate activator showed the crystalline phase of gypsum, indicating that the sulfate activator was not fully reacted at 1 d. When the age was 3 d, the main crystal phases were quartz and calcite; there was no gypsum diffraction peak, indicating that the sulfate activator had completely reacted within 3 d.

AFt did not appear at different ages, mainly for the following reasons: in a highly alkaline environment, AFt is unstable and is easily transformed into a single-sulfur calcium hydrate phase, and $Ca^{2+}$ is consumed in large quantities [31, 32]. The formation of calcite is caused by C-S-H carbonisation [33]. The main reason for the evident quartz diffraction peak was that the stone

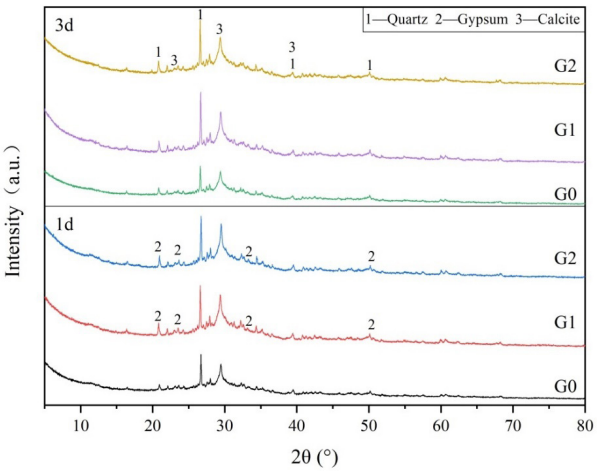


Figure 10. XRD patterns for the 1-d and 3-d MSGCC with the different gypsum contents.

powder and other materials did not react completely. The strength of the multicomponent composite cementing material was primarily provided by C-S-H and N-A-S-H; the addition of stone powder reduced the production of the two gels and resulted in a decrease in the mechanical properties.

## CONCLUSIONS

(1) The composite cement material prepared by the response surface method showed high flexural and compressive strengths, and the 28-d compressive strength was above 65 MPa. By fitting the test data, a multicomponent regression model was established for the prediction, and the optimal ratios were 14.45 % for stone powder and 0.91 % for gypsum. The model showed strong reliability and applicability. Additionally, it was found that when the gypsum content was 1.25 %, the bending strength was promoted to some extent.

(2) The mechanism for the combined alkali and sulfate activation was analysed by determining the hydration heat and XRD patterns. The results showed that with the addition of the sulfate activator, the hydration heat release rate and hydration heat release gradually decreased. The hydration products of the 1-d and 3-d MSGCC were quartz, gypsum, and calcite, and the crystal phase of gypsum disappeared at 3 d.

(3) With alkali-activation, an increase in the sulfate activator content changed the hydration products formed from the strength source of the multicomponent composite cementitious materials, and it affected the hydration reaction process of the system. Therefore, the use of common alkali activators and sulfate activators improved the particle surface structural damage and repolymerisation environment after different periods of hydration and structure formation processes and built a good hydration product microstructure.

Acknowledgements

*We wish to thank the Natural Science Foundation of Zhejiang Province (LZ22E080003), Science and Technology Project of Zhejiang Provincial Department of Transport (202225), Ningbo Transportation Science and Technology Project (202007), and Natural Science Foundation of Zhejiang Province (LY20E080002).*

## REFERENCES

1. Ramadji C., Messan A., Prud'Homme E. (2020) : Influence of granite powder on physico-mechanical and durability properties of mortar. *Materials, 13*(23), 5406. Doi: 10.3390/ma13235406
2. Liu S., Yan P. (2010): Effect of limestone powder on microstructure of concrete. *Journal of Wuhan University of Technology-Mater. Sci. Ed., 25*(2), 328-331. Doi: 10.1007/s11595-010-2328-5
3. GB/T 14684-2011 (2011). *Sand for construction.* Beijing: Standards Press of China.
4. Chi M., Huang R. (2013): Binding mechanism and properties of alkali-activated fly ash/slag mortars. *Construction and Building Materials, 40*, 291-298. Doi: 10.1016/j.conbuildmat.2012.11.003
5. Zhou S, Tan C, Gao Y, et al. (2021): One-part alkali activated slag using $Ca(OH)_2$ and $Na_2CO_3$ instead of NaOH as activator: more excellent compressive strength and microstructure. *Materials Research Express, 8*(8), 85501. Doi: 10.1088/2053-1591/ac16f4
6. Komljenović M. M., Baščarević Z., Marjanović N., Nikolić V. (2012): Decalcification resistance of alkali-activated slag. *Journal of Hazardous Materials, 233*, 112-121. Doi: 10.1016/j.jhazmat.2012.06.063
7. Koplík J., Kalina L., Másilko J., Šoukal F. (2016): The characterization of fixation of Ba, Pb, and Cu in alkali-activated fly ash/blast furnace slag matrix. *Materials, 9*(7), 533. Doi: 10.3390/ma9070533
8. Park S. M., Jang J. G., Lee N. K., Lee H. K. (2016): Physicochemical properties of binder gel in alkali-activated fly ash/slag exposed to high temperatures. *Cement and Concrete Research, 89*, 72-79. Doi: 10.1016/j.cemconres.2016.08.004
9. Lim Y. Y., Pham T. M., Kumar J. (2021): Sustainable alkali activated concrete with fly ash and waste marble aggregates: Strength and Durability studies. *Construction and Building Materials, 283*, 122795. Doi: 10.1016/j.conbuildmat.2021.122795
10. Song K. I., Song J. K., Lee B. Y., Yang K. H. (2014): Carbonation characteristics of alkali-activated blast-furnace slag mortar. *Advances in Materials Science and Engineering, 2014*, 326458. Doi:10.1155/2014/326458
11. Nguyen H. A. (2018): Utilization of commercial sulfate to modify early performance of high volume fly ash based binder. *Journal of Building Engineering, 19*, 429-433. Doi: 10.1016/j.jobe.2018.06.001
12. Sivapullaiah P. V., Baig M. A. A. (2011): Gypsum treated fly ash as a liner for waste disposal facilities. *Waste Management, 31*(2), 359-369.Doi: 10.1016/j.wasman.2010.07.017
13. Rashad A. M., Bai Y., Basheer P. A. M., Milestone N. B., Collier N. C. (2013): Hydration and properties of sodium sulfate activated slag. *Cement and Concrete Composites, 37*, 20-29. Doi: 10.1016/j.cemconcomp.2012.12.010
14. Mobasher N., Bernal S. A., Provis J. L. (2016): Structural evolution of an alkali sulfate activated slag cement. *Journal of Nuclear Materials, 468*, 97-104. Doi: 10.1016/j.jnucmat.2015.11.016
15. Dakhane A., Tweedley S., Kailas S., Marzke R., Neithalath N. (2017): Mechanical and microstructural characterization of alkali sulfate activated high volume fly ash binders. *Materials & Design, 122*, 236-246. Doi: 10.1016/j.matdes.2017.03.021
16. Qiu Y. B., Wang Q. P. (2013): Study on the pozzolanic activity of fly ash activated by $Na_2SO_4$. *Materials Review, 27*(12), 120-121.
17. Lv Q. F., Wang Z. S., Gu L. Y., Chen Y., Shan X. K. (2020): Effect of sodium sulfate on strength and microstructure of alkali-activated fly ash based geopolymer. *Journal of Central South University, 27*(6), 1691-1702.Doi: 10.1007/s11771-020-4400-4
18. Zhang L., Chen B. (2017): Hydration and properties of slag cement activated by alkali and sulfate. *Journal of Materials in Civil Engineering, 29*(9), 04017091.Doi: 10.1061/(ASCE)MT.1943-5533.0001879
19. Wang J. W., Wang W. (2019): Response Surface Based Multi-objective Optimization of Basalt Fiber Reinforced Foamed Concrete. *Materials Reports, 33*(24), 4092-4097.
20. Gao Y., Xu J., Luo X., Zhu J., Nie L. (2016) : Experiment research on mix design and early mechanical performance of alkali-activated slag using response surface methodology (RSM). *Ceramics International, 42*(10), 11666-11673.Doi: 10.1016/j.ceramint.2016.04.076
21. Sahu S. S., Gandhi I. S. R. (2021): Studies on influence of characteristics of surfactant and foam on foam concrete behaviour. *Journal of Building Engineering, 40*, 102333. Doi: 10.1016/j.jobe.2021.102333
22. Zhang L. F., Song S. S., Liang Q. S.(2020): Effect of gypsum content on properties of alkali-activated slag cement mortar. *Applied Chemical Industry, 49*(09), 2168-2172.
23. Vaičiukynienė D., Nizevičienė D., Kielė A., Janavičius E., Pupeikis D. (2018): Effect of phosphogypsum on the stability upon firing treatment of alkali-activated slag. *Construction and Building Materials, 184*, 485-491.Doi: 10.1016/j.conbuildmat.2018.06.213
24. Muthukumar M., Mohan D. (2004): Studies on polymer concretes based on optimized aggregate mix proportion. *European Polymer Journal, 40*(9), 2167-2177.Doi: 10.1016/j.eurpolymj.2004.05.004
25. Geng D. X., Hu Y. C., Liao Y. Q., et al. (2021): Performance of Synchronous Grouting Material for Slurry Shield Based on Response Surface Method. *Science Technology and Engineering, 21*(15), 6479-6486.
26. Liu J., Hu L., Tang L., Zhang E. Q., Ren J. (2020): Shrinkage behaviour, early hydration and hardened properties of sodium silicate activated slag incorporated with gypsum and cement. *Construction and Building Materials, 248*, 118687. Doi: 10.1016/j.conbuildmat.2020.118687
27. Zhang K., Liu F., Yue Q., Feng J. (2020): Effect of granite powder on properties of concrete. *Asia-Pacific Journal of Chemical Engineering, 15*, e2468. Doi: 10.1002/apj.2468
28. Li Z. F., Chen J. P., Yang L., et al. (2021): Influence mechanism of limestone powder on red mud-based grouting

material. *Chinese Journal of Engineering, 43*(6), 768-777. doi: 10.13374/j.issn2095-9389.2020.12.01.005

29. Zhang R. L., Chen Y. Q., Liu S. T., et al. (2016): Influence of stone powder content on performance of machine-made sand concrete. *Concrete, 2016*, 1.
30. Yang N. R. (2018). Non-tradition Cementitious Materials Chemistry. Wuhan University of Technology Press.
31. Ma P. F., Li S., Chen B. J., et al. (2020) : Research on contractility of alkali activated slag mortar. *Inorganic Chemicals Industry, 52*(10), 145-150.
32. Yuan S. H., Shen X. W. (2017): Experimental Study on Shrinkage Compensation Performance of Alkali-activated Slag Concrete. *Bulletin of the Chinese Ceramic Society, 36*(9), 2987-2993.
33. Ma Q. M., Huan L. P., Niu Z. L., et al. (2008): Effect of Alkali Concentration and Modulus of Alkaline Activator on the Compressive Properties and Hydration Products of Alkali Activated Slag Cementitious Materials. *Bulletin of the Chinese Ceramic Society, 37*(06), 2002-2007.